analytical chemistry

pubs.acs.org/ac Article

Target-Initiated Cascade Signal Amplification Lights up a G-Quadruplex for a Label-Free Detection of Circular Ribonucleic Acids

Shu-hua Wei,[§] Meng Liu,[§] Juan Hu,* and Chun-yang Zhang*

Cite This: *Anal. Chem.* 2022, 94, 9193−9200 Read Online

ACCESS | Metrics & More | Article Recommendations | Supporting Information

ABSTRACT: Circular ribonucleic acids (circRNAs) are a type of RNA that originates through back-splicing events from linear primary transcripts. CircRNAs display high structural resistance and tissue specificity. Accurate quantification of the circRNA expression level is of vital importance to disease diagnosis. Herein, we construct a label-free fluorescent biosensor for ultrasensitive analysis of circRNAs based on the integration of target-initiated cascade signal amplification strategy with a light-up G-quadruplex. This assay involves only one assistant probe that targets the circRNA-specific back-splice junction. When circRNA is present, it hybridizes with the assistant probe to initiate the duplex-specific nuclease (DSN)-catalyzed cyclic cleavage reaction, producing abundant triggers with 3′OH termini. Then, terminal deoxynucleotidyl transferase (TdT) catalyzes the addition of dGTP and dATP at the 3′-OH termini of the resultant triggers to obtain abundant long G-rich DNA sequences that can form efficient G-quadruplex products. The addition of Thioflavin T (ThT) can light up G-quadruplex, generating an enhanced fluorescence. This assay may be performed isothermally without the involvement of any nucleic acid templates, exogenous primers, and specific labeled probes. Importantly, this biosensor can discriminate target circRNA from one-base mismatched circRNA and exhibits good performance in human serum. Moreover, it can accurately detect circRNA in cancer cells at a single-cell level and even differentiate the circRNA levels in the tissues of healthy persons and nonsmall cell lung cancer (NSCLC) patients, with promising applications in circRNA-related cancer diagnosis and therapeutics.

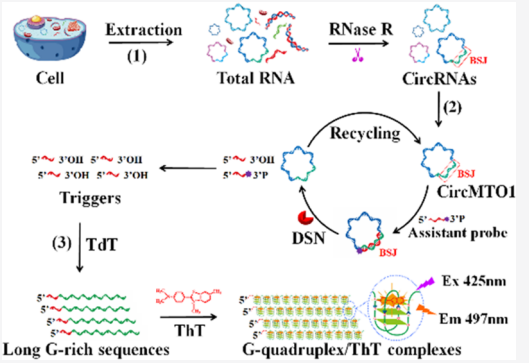

Circular RNAs (circRNAs) are characterized by high stability, long half-life, and high specificity of tissue/cell expression.[1,2] CircRNAs can function as sponges of microRNAs and RNA-binding proteins[3] as well as the dynamic scaffolds that modulate protein−protein interactions[4] and regulate the translation/transcription[5] and alternative splicing events.[6] CircRNAs are deeply involved in human cancers and have been identified as the oncogenes due to their upregulation in various solid tumors such as lung cancer,[7] cervical cancer,[8] colorectal cancer,[9] and hepatocellular carcinoma.[10] Moreover, circRNAs are downregulated in human glioblastoma[11] and gastric cancer,[12] suggesting their tumor-suppressive function. Aberrant circRNAs are involved in cardiovascular diseases,[13] diabetes mellitus,[14] and neurological disorders such as Alzheimer's disease,[15,16] and may function as the promising diagnostic, therapeutic, and prognostic biomarkers.[9,17,18] Therefore, the accurate identification and detection of cancer-related circRNAs have become increasingly important in clinical diagnosis.

Available technologies for the detection of circRNAs include microarray analysis,[19] RNA sequencing,[20] Northern blotting,[20,21] reverse transcription polymerase chain reaction (PCR),[20−22] droplet digital PCR,[23] ligation-based PCR,[24] and electrochemical measurement.[25,26] However, they usually suffer from some limitations such as the requirement of specialized equipment (for RNA sequencing and droplet digital PCR), ample computational power (for RNA sequencing), radioactively labeled probes (for Northern blotting), divergent primers design, and high-precision temperature control (for PCR), labor-intensive (for microarray analysis, RNA sequencing, and Northern blotting), and low sensitivity (for Northern blotting, ligation-based PCR, and electrochemical measurement).[19−26] Alternatively, isothermal amplification approaches including hybridization chain reaction,[27] rolling circle amplification,[28,29] and cyclic enzymatic amplification[30] have shown great potential in circRNA assay. Despite their advantages of isothermal and high amplification efficiency without the need for tedious procedures,[31−34] they often require specific reverse transcription primers, DNA templates,

Received: April 30, 2022
Accepted: June 3, 2022
Published: June 15, 2022

https://doi.org/10.1021/acs.analchem.2c01901
Anal. Chem. 2022, 94, 9193−9200

Scheme 1. Schematic Illustration of the Label-Free Detection of CircRNA Based on the Integration of Target-Initiated Cascade Signal Amplification Strategy with a Light-up G-Quadruplex

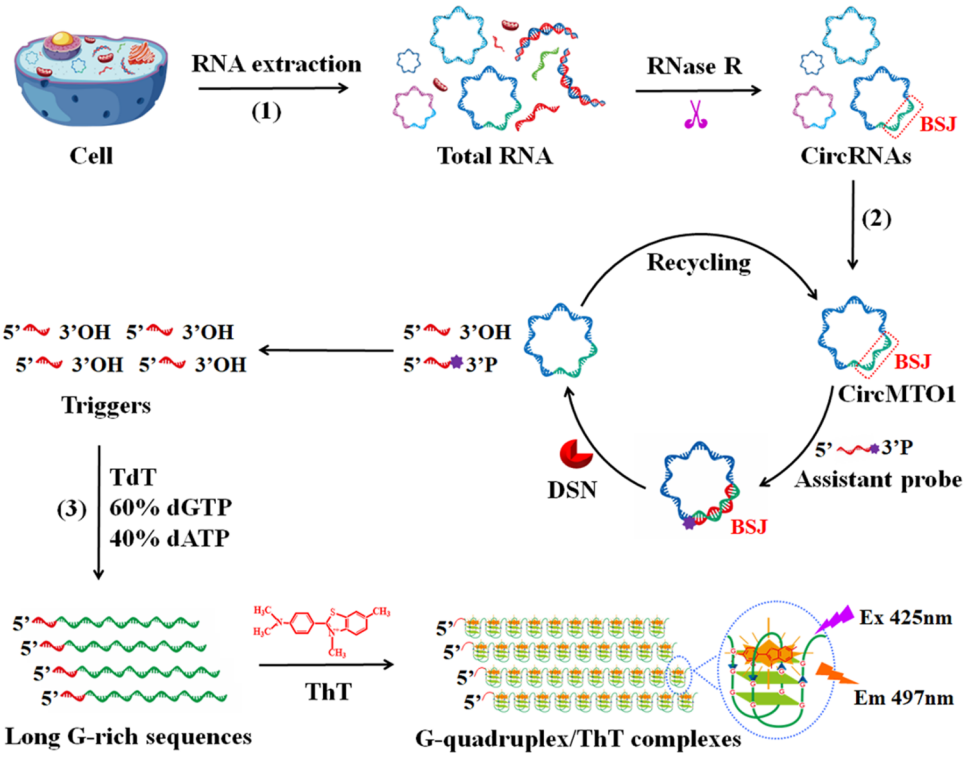

and fluorophore/quencher-labeled hairpin probes.[27−30] Consequently, new highly efficient methods for simple and sensitive analysis of circRNA biomarker in real samples are highly desirable.

In contrast to the detection of linear nucleic acids (e.g., long noncoding RNAs and miRNAs),[35−39] the enrichment and identification of circRNAs remain a great challenge due to their lack of capping and poly-adenylation, ultralong sequence, structure complexity, and the lower levels than linear species.[1,40] Herein, we construct a label-free fluorescent biosensor for an ultrasensitive analysis of circRNAs based on the integration of a target-initiated cascade signal amplification strategy with a light-up G-quadruplex. The combination of G-quadruplex with small fluorogenic molecules may function as signal indicators for biosensing.[41−44] This assay does not need any complicated steps, large sample consumption, and specific labeled probes and possesses distinct features of simple operation, high sensitivity, and excellent specificity. Moreover, it can accurately detect circRNAs in cancer cells and even differentiate between cancer cells and normal cells.

EXPERIMENTAL SECTION

Materials. Details about all materials are given in the Supporting Information, and all oligonucleotide sequences are given in Tables S1 and S2.

Synthesis and Purification of CircRNA. CircRNA was prepared by ligation reaction in 20 μL of a mixture containing 1× ligation buffer, 200 nM linear RNA-1, 20 U of RiboLock RNase inhibitor, 200 nM guide RNA, and 2 U of T4 RNA ligase 2. The one-base mismatched circRNA was prepared using one-base mismatched linear RNA-1. Prior to the addition of ligase, linear RNA-1, guide RNA, ligation buffer, and RNase-free water were reacted for 3 min at 95 °C, followed by cooling to room temperature. After the addition of ligase, the mixture was reacted at 37 °C for 90 min to form circRNAs, followed by inactivation at 80 °C for 5 min. Then, 2 U of RNase R and 1× RNase R reaction buffer were added and reacted at 37 °C for 10 min to remove the excess linear RNAs, followed by inactivation for 10 min at 70 °C. The obtained circRNAs were subjected to the measurements.

Target-Initiated DSN/TdT-Assisted Cascade Signal Amplification. For a typical DSN-catalyzed cleavage recycling reaction, 100 nM assistant probe, 20 U of RNase inhibitor, 1× TdT buffer, and different concentrations of circRNA were reacted for 20 min at room temperature to produce the DNA/circRNA heteroduplex. Then, 0.05 U of DSN was added and reacted for 35 min at 60 °C, followed by heat inactivation at 80 °C for 20 min. Subsequently, the reaction mixture was incubated with 4 U of TdT, 0.06 μL of 100 mM dATP, and 0.09 μL of 100 mM dGTP with a total volume of 20 μL at 37 °C for 40 min to perform the TdT-mediated G-quadruplex synthesis reaction, followed by inactivation for 20 min at 80 °C.

Fluorescence Measurement. FLS1000 (Edinburgh Instruments, U.K.) with an emission slit of 5.0 nm was used to obtain the fluorescence emission spectra of ThT for data analysis, with error bars indicating the standard deviations of three experiments.

Gel Electrophoresis Analysis. We used 12% native polyacrylamide gel electrophoresis (PAGE) to verify the product of circRNA-initiated DSN/TdT-assisted cascade signal amplification. The product was stained with SYBR Gold and then analyzed in 1× TBE buffer (0.2 mM EDTA, 9 mM boric acid, 9 mM Tris−HCl, pH 7.9) for 60 min at a 110 V constant voltage. The images of gel electrophoresis were

https://doi.org/10.1021/acs.analchem.2c01901
Anal. Chem. 2022, 94, 9193−9200

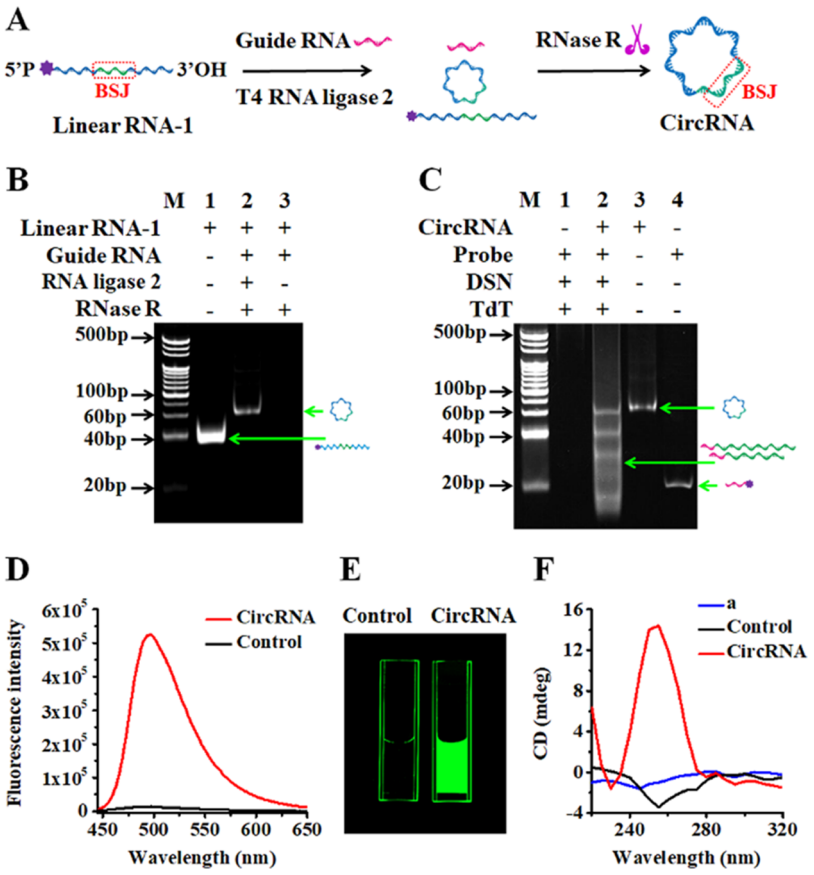

Figure 1. (A) Synthesis of circRNA using a linear RNA-1 and a guide RNA. (B) Verification of the synthesized circRNA product by PAGE. Lane M, 20 bp DNA ladder marker; lane 1, linear RNA-1; lane 2, linear RNA-1 + guide RNA + T4 RNA ligase 2 + RNase R; lane 3, linear RNA-1 + guide RNA + RNase R. The 200 nM linear RNA-1, 200 nM guide RNA, 2 U of RNase R, and 2 U of T4 RNA ligase 2 were used in the experiments. (C) PAGE analysis of circRNA-initiated DSN/TdT-assisted cascade signal amplification product. Lane M, 20 bp DNA ladder marker; lane 1, assistant probe + DSN + TdT; lane 2, circRNA + assistant probe + DSN + TdT; lane 3, circRNA; lane 4, assistant probe. The 100 nM circRNA and 100 nM assistant probe were used in the experiments. (D) Fluorescence emission spectra in the absence (control, black line) and presence (red line) of 50 nM circRNA. (E) Fluorescence images of reaction products in the absence (control, left) and presence (right) of 50 nM circRNA. The 100 nM assistant probe and 4 U of TdT were used in the experiments. (F) Circular dichroism spectroscopy in the absence (control, black line) and presence (red line) of 50 nM circRNA. CircRNA alone is shown in line a (blue line).

visualized by a Bio-Rad ChemiDoc MP Imaging system (Hercules, CA).

Circular Dichroism Measurement. We used circular dichroism (CD) spectroscopy to verify the formation of circRNA-induced G-quadruplex/ThT complexes. Circular dichroism spectra were collected using a MOS-500 multifunctional circular dichroism spectrometer (France).

Preparation of Total RNA. The cultured cells (see the Supporting Information) were counted using a Countstar cell counter. CircRNAs were extracted from cells using a total RNA extractor (Trizol). A miRNeasy FFPE kit (Qiagen, Germany) was used to extract the total RNA from the lung tissues of healthy persons and NSCLC patients, respectively. The concentration of the total RNA was measured using a Nanodrop 2000C spectrophotometer (Thermo Scientific).

RESULTS AND DISCUSSION

Principle of CircRNA Assay. Scheme 1 illustrates the principle of circRNA assay. We used circRNA mitochondrial tRNA translation optimization 1 (circMTO1, Table S1) as a model circRNA, which originates from exons of MTO1 located on chromosome 6q13.[45−47] This circRNA assay involves only one assistant probe that can hybridize with the back-splice junction (BSJ) of circMTO1. The BSJ region is the only region of circMTO1 distinct from its corresponding linear RNA.[1,48] To prevent the nonspecific amplification, the 3′ terminus of the assistant probe is modified with the phosphate group (3′P). The assay contains the following three steps: (1) circRNA extraction from cells, (2) DSN-catalyzed cyclic cleavage of assistant probes, and (3) TdT-mediated G-quadruplex synthesis reaction. To identify exonic circMTO1 on a genomic scale, total RNA is isolated from the cultured cell lines. Then, ribonuclease R (RNase R) digests linear RNAs regardless of secondary structure, leaving circular RNAs unaffected.[49] The natural circRNAs selected from total RNA are subjected to measurement. In the presence of circMTO1, an assistant probe binds with the BSJ sequence within circMTO1 to form the DNA/circRNA heteroduplex. Subsequently, an assistant probe in the DNA/circRNA heteroduplex is selectively cleaved by DSN into DNA fragments, releasing the intact circRNA and the triggers with 3′OH termini. The released circRNA can hybridize with the new assistant probe to form the DNA/circRNA heteroduplex, initiating the DSN-catalyzed cyclic cleavage of assistant probes, generating abundant triggers with 3′OH termini. With the assistance of TdT, the incubation of the resultant triggers with

https://doi.org/10.1021/acs.analchem.2c01901
Anal. Chem. 2022, 94, 9193−9200

60% dGTP and 40% dATP obtains abundant long G-rich DNA sequences with different lengths. The G-quadruplex products can form a stable fluorescent complex with Thioflavin T (ThT) to produce an improved fluorescence signal. When circMTO1 is absent, no cleavage of assistant probes occurs. Consequently, no trigger with the 3′OH terminus is available for the TdT-mediated G-quadruplex synthesis reaction, and no fluorescence signal is measured. Notably, this strategy has the following distinct advantages: (1) RNase R treatment not only purifies circMTO1 but also efficiently suppresses the undesirable background because the covalent loop structure of circRNAs protects them from exonuclease (e.g., RNase R)-mediated degradation.[49] (2) DSN-catalyzed cyclic cleavage of assistant probes facilitates the continuous production of abundant triggers with 3′OH termini, resulting in significant signal amplification and a reduced background signal. Notably, DSN can cleave the assistant probe in DNA/circRNA heteroduplex without the involvement of a specific recognition sequence,[50] but it is inactive toward the assistant probe alone. Moreover, DSN can differentiate perfectly from nonperfectly matched DNA/circRNA heteroduplex with even one mismatch. (3) TdT-mediated G-quadruplex synthesis reaction induces high amplification efficiency and ultralow background without the requirement of exogenous primers. The unique sequence-independent extension property of TdT can produce abundant long G-rich DNA sequences through encoding gene to form the G-quadruplexes.[51] (4) Introduction of ThT induces an enhanced fluorescence without the involvement of specific labeled probes. ThT is a small fluorogenic molecule, and it selectively recognizes G-quadruplex structure instead of other structures (e.g., assistant probe) to generate a lighting-up fluorescence.[52] Notably, the whole assay can be implemented without the requirement of varying reaction temperature, tedious experimental steps, and large sample consumption, providing a simple platform for label-free and ultrasensitive detection of circRNA.

Assay Feasibility. To mimic the circMTO1-initiated DSN/TdT-assisted cascade signal amplification, we synthesized a circRNA using a linear RNA-1 and a guide RNA (Figure 1A and Table S2). The linear RNA-1 is modified with 5′P and 3′OH ends containing two RNA sequences and a back-splice junction (BSJ) site sequence of target circMTO1. When guide RNA is present, it hybridizes with either side of linear RNA-1, making the ends of linear RNA-1 to be specifically ligated by T4 RNA ligase 2. The excess linear RNA-1 and guide RNA are degraded by RNase R to efficiently suppress the undesirable background. The synthesized circRNA are subjected to the measurements.

The T4 RNA ligase 2-catalyzed synthesis of circRNA is analyzed by 12% PAGE. Only a 52-nt band of linear RNA-1 is detected in the presence of linear RNA-1 (Figure 1B, lane 1). In the presence of linear RNA-1 + guide RNA + T4 RNA ligase 2 + RNase R, one characteristic 52-nt band of circRNA is observed (Figure 1B, lane 2). The 52-nt band of circRNA (Figure 1B, lane 2) migrates more slowly than the 52-nt band of linear RNA-1 (Figure 1B, lane 1), suggesting the successful synthesis of circRNA. Since the linear RNA-1 and guide RNA are quickly digested by RNase R, no RNA band is observed in the presence of linear RNA-1 + guide RNA + RNase R (Figure 1B, lane 3).

The product of circRNA-initiated DSN/TdT-assisted cascade signal amplification is electrophoresed in a 12% PAGE. CircRNA generates a 52-nt band (Figure 1C, lane 3), and the assistant probe generates a 30-nt band (Figure 1C, lane 4). Upon the addition of DSN and TdT, the bands of amplification products with different lengths are detected in the presence of circRNA + assistant probe + DSN + TdT (Figure 1C, lane 2), but no band is detected in the presence of assistant probe + DSN + TdT (Figure 1C, lane 1). These results indicate that circRNA can induce DSN-catalyzed cyclic cleavage reaction and TdT-mediated G-quadruplex synthesis reaction.

We further carried out fluorescence measurements. When target circRNA is absent, no significant fluorescence spectrum is detected (Figure 1D, black line), indicating that neither DSN-catalyzed cleavage recycling reaction nor TdT-mediated G-quadruplex synthesis reaction occurs due to lack of target circRNA. In contrast, when target circRNA is present, the amplification product specifically binds to ThT to produce a remarkable fluorescence with a maximum wavelength of 497 nm (Figure 1D, red line). The F/F_0 value is calculated to be 18.4, where F_0 and F are the ThT signals in the absence and presence of circRNA, respectively. The result is validated by the distinct green fluorescence image of G-quadruplex/ThT complexes in response to target circRNA (Figure 1E). In addition, the formation of G-quadruplex/ThT complexes is confirmed by circular dichroism (CD) spectroscopy. There is no obvious peak in response to either circRNA alone (Figure 1F, blue line) or the absence of circRNA (Figure 1F, black line), but a distinct positive peak at 260 nm is detected in response to circRNA, suggesting the formation of the circRNA-induced G-quadruplex/ThT complexes.[42]

To further confirm the high amplification efficiency of circRNA-initiated DSN/TdT-assisted cascade signal amplification, we used a linear RNA-2 modified with 3′-phosphate (3′P) to investigate the process of DSN/TdT-assisted cascade signal amplification (Figures S1 and S2). The F/F_0 value is calculated to be 12.8 in response to linear RNA-2 (Figure S3), which is much lower than that generated by circRNA (18.4), suggesting that circRNA possesses higher amplification efficiency as a result of the higher cleavage efficiency of DSN toward circRNA than toward linear RNA-2 (Figure S4).

Detection Sensitivity. We studied the sensitivity of circRNA under optimal reaction conditions (Figures S5−S8). As the concentration of circRNA (C) increases, the ThT fluorescence intensities (F) improve correspondingly (Figure 2A) with a large dynamic range over 7 orders of magnitude from 1×10^{-16} to 1×10^{-9} M. The correlation equation is $F = 847230.89 + 49544.23 \lg C$ ($R^2 = 0.9995$). The LOD is determined to be 3.03×10^{-17} M. This method is simple, highly sensitive, label free, and superior to the reported methods (Table S3). The sensitivity of this method is 5 orders of magnitude higher than that of fluorescence assay based on cyclic enzymatic amplification (1 pM),[30] 4 orders of magnitude higher than that of electrochemical method (0.22 pM),[25] and 2 orders of magnitude higher than that of ligation-mediated PCR (1 fM).[24] The ultrahigh sensitivity is mainly ascribed to the following factors: (1) DSN-catalyzed cyclic cleavage of assistant probe releases large amounts of triggers, greatly improving amplification efficiency. (2) TdT-mediated G-quadruplex synthesis reaction produces abundant long G-rich DNA sequences, resulting in significant ThT fluorescence signal amplification. Notably, the reaction time of circRNA-initiated DSN/TdT-assisted cascade signal amplification is very short (2 h) compared with the reported methods (Table S3) such as the electrochemical measurement (11.5 h).[25]

https://doi.org/10.1021/acs.analchem.2c01901
Anal. Chem. 2022, 94, 9193−9200

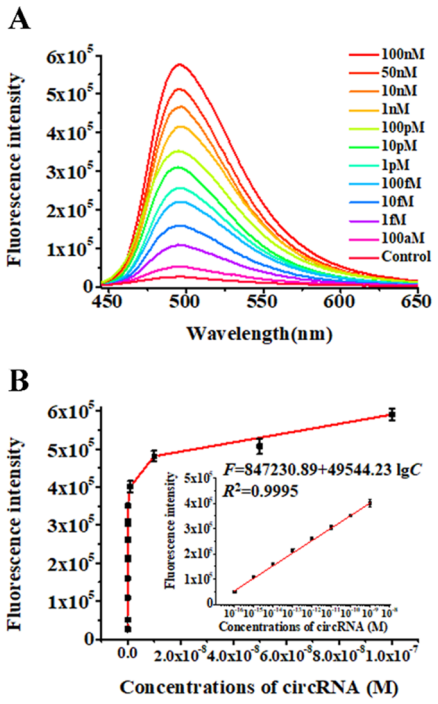

Figure 2. (A) Fluorescence emission spectra generated by various concentrations of circRNA. (B) Variance in the fluorescence intensity with the circRNA concentration. Inset displays the linear dependence of fluorescence intensity upon the logarithm of circRNA concentration from 100 aM to 1 nM. The 100 nM assistant probe and 4 U of TdT were used in this research.

Detection Specificity. A significant challenge for circRNA analysis is the discrimination of a single-base mismatch in circRNA. We designed one-, two-, and three-base mismatched assistant probes and one-base mismatched circRNA. As shown in Figure 3, the fluorescence signal generated by circRNA + assistant probe (Figure 3, red column) is much higher than those generated by circRNA + one-base mismatched assistant probe (Figure 3, column a), circRNA + two-base mismatched assistant probe (Figure 3, column b), circRNA + three-base mismatched assistant probe (Figure 3, column c), assistant probe + one-base mismatched circRNA (Figure 3, column d), and the control without circRNA (Figure 3, black column). Notably, the fluorescence intensity produced by circRNA + assistant probe is 12.5-, 15.5-, 19.3-, and 19.2-fold higher than that produced by one-, two-, and three-base mismatched assistant probe + circRNA and one-base mismatched circRNA + assistant probe, respectively. These results suggest that this method possesses excellent specificity and can even discriminate single-base mutation.

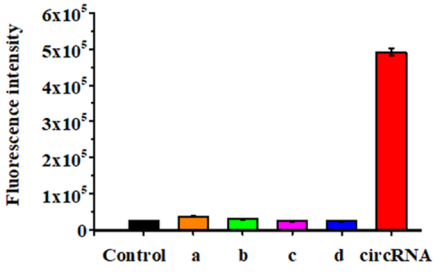

Figure 3. Measurement of fluorescence intensity generated by circRNA + one-base mismatched assistant probe (a, orange column), circRNA + two-base mismatched assistant probe (b, green column), circRNA + three-base mismatched assistant probe (c, magenta column), one-base mismatched circRNA + assistant probe (d, blue column), circRNA + assistant probe (red column), and assistant probe without circRNA (control, black column). The circRNA concentration is 50 nM, and the concentration of each assistant probe is 100 nM.

Detection of CircRNA in Serum. We further measured circRNA spiked in 10% human serum. Figure 4 displays the calibration curve of fluorescence intensity (F) vs the concentration of spiked circRNA (C) from 1×10^{-16} to 1×10^{-9} M, with the equation being $F = 876477.98 + 52631.71$ lgC ($R^2 = 0.9989$). The LOD is determined to be 7.52×10^{-17} M, consistent with that obtained in Figure 2B (3.03×10^{-17} M). In addition, we determined the recovery ratio (Table S4). A recovery ratio of 99.80−100.98% with a relative standard deviation of 2.51−5.18% is obtained. These results suggest that this method exhibits good reliability and reproducibility even in a complex biological matrix.

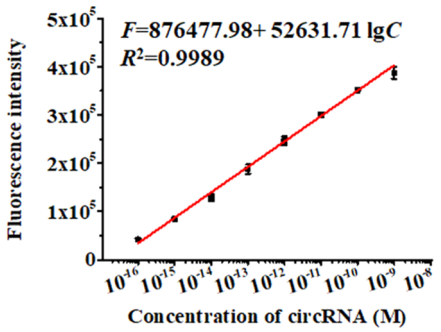

Figure 4. Linear dependence of fluorescence intensity upon the logarithm of circRNA concentration in 10% human normal serum.

Profiling of Cellular CircMTO1 Expression. The circMTO1 biomarker is valuable for the early phase diagnosis and therapeutics of cancers.[45] We investigated the feasibility of this method for cellular circMTO1 detection. We tested five human cell lines including human normal liver cells (LO2 cells), hepatocellular carcinoma cell lines (HepG2 cells), breast cancer cell lines (MCF-7 cells), lung adenocarcinoma cell line (A549 cells), and cervical carcinoma cell line (HeLa cells), and we detected the emission spectra generated by extracts of 100,000 cells (Figure S9). Notably, the proposed method exhibits excellent selectivity toward cellular circMTO1 with no response to nonspecific proteins and peptides (Figure S10). As shown in Figure 5A, the fluorescence intensity generated by normal liver LO2 cells (Figure 5A, blue column) is higher than that generated by HepG2 cells (Figure 5A, green column), suggesting that circMTO1 is downregulated in hepatocellular carcinoma cells, consistent with the previous report.[45] The lowest fluorescence intensity is detected in A549 cells (Figure 5A, orange column), indicating that circMTO1 is significantly downregulated in lung adenocarcinoma cells (previous RT-qPCR analysis).[53] The highest fluorescence intensity is detected in HeLa cells (Figure 5A, red column), indicating the upregulation of circMTO1 in cervical cancer cells, consistent with the previous RT-qPCR analysis.[46] The expression of circMTO1 decreases in the order of HeLa cells > LO2 cells > MCF-7 cells > HepG2 cells > A549 cells, consistent with the result obtained by rolling circle amplification-based fluorescence imaging.[28] In addition, we

https://doi.org/10.1021/acs.analchem.2c01901
Anal. Chem. 2022, 94, 9193−9200

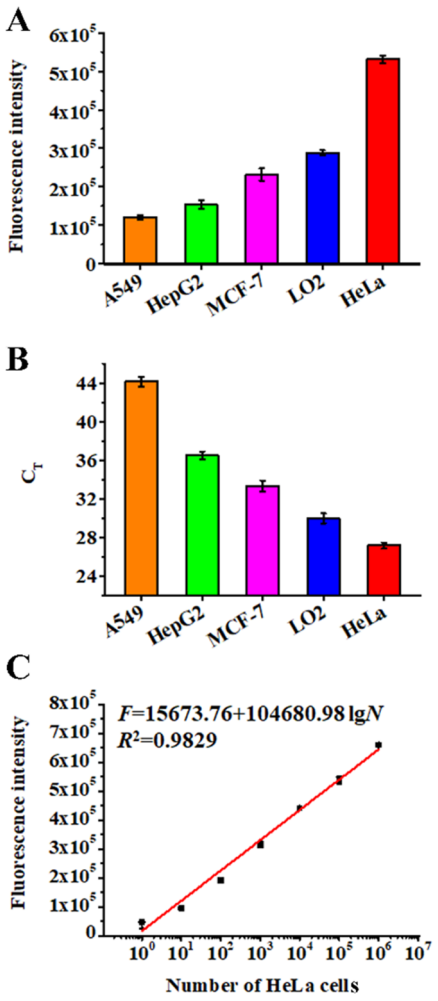

Figure 5. (A) Measurement of fluorescence intensity generated by A549 cells (orange column), HepG2 cells (green column), MCF-7 cells (magenta column), LO2 cells (blue column), and HeLa cells (red column). A total of 1×10^5 cells were used for each experiment. (B) Threshold cycle (C_T) value of circMTO1 measured by RT-qPCR in response to A549 cells (orange column), HepG2 cells (green column), MCF-7 cells (magenta column), LO2 cells (blue column), and HeLa cells (red column). 1×10^5 cells were used for each experiment. (C) Linear dependence of fluorescence intensity upon the logarithm of HeLa cell number from 1 to 1×10^6 cells.

compared our results with those obtained by the RT-qPCR analysis (Figure S11). Figure 5B shows that the threshold cycle (C_T) values of different cell lines increases in the order of HeLa cells < LO2 cells < MCF-7 cells < HepG2 cells < A549 cells. There is good agreement between the proposed method (Figure 5B) and RT-qPCR analysis (Figure S11).

We further detected the fluorescence intensity induced by various numbers of HeLa cells. As the number of HeLa cells increases, the ThT fluorescence intensities improve correspondingly. Figure 5C displays the calibration curve of fluorescence intensity (F) vs various numbers of HeLa cells (N) from 1 to 1,000,000 cells, with the equation being $F = 15673.76 + 104680.98 \lg N$ ($R^2 = 0.9829$). The LOD is determined to be 1 cell.

Measurement of CircMTO1 in Clinical Tissues. To further confirm the feasibility of this method for real clinical samples, we detected the circMTO1 levels in the tissues of healthy persons and nonsmall cell lung cancer (NSCLC) patients (Figure 6). In comparison with that in the tissues of nine healthy persons, circMTO1 expression levels are

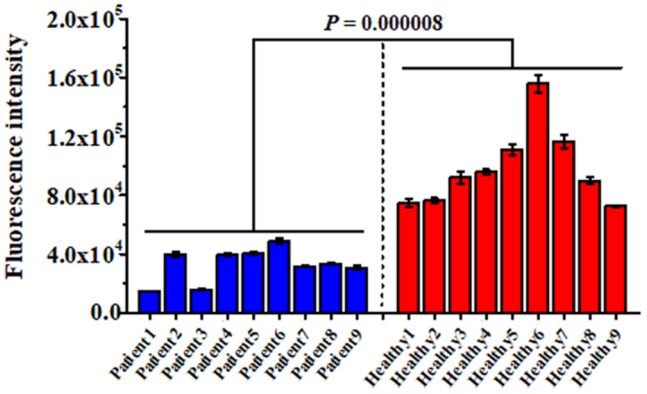

Figure 6. Measurement of circMTO1 expression level in the tissues of NSCLC patients (blue column) and healthy lung tissues (red column). Two hundred fifty nanograms of total RNA extract was measured for each experiment.

significantly downregulated in nine NSCLC patient tissues ($P < 0.0001$). The average fluorescence signal generated by healthy person tissues is 98214.81 ± 24961.21, which is threefold higher than that generated by the tissues of NSCLC patients (32700.11 ± 10645.85), suggesting that the dysregulation of circMTO1 is closely related to NSCLC, consistent with the previous research.[53]

CONCLUSIONS

We have constructed a label-free fluorescent biosensor for an ultrasensitive analysis of circRNAs based on the integration of a target-initiated cascade signal amplification strategy with a light-up G-quadruplex. This biosensor has significant features: (1) The target-initiated DSN/TdT-assisted cascade signal amplification significantly improves the sensitivity and reduces the background signal. (2) In comparison with the reported isothermal amplifications,[28,29] the TdT-mediated G-quadruplex synthesis endows this biosensor with excellent simplicity without the involvement of any DNA templates and exogenous primers. (3) The use of G-quadruplex/ThT complexes as a signal producer does not require specific labeled probes,[27] enabling label-free detection of circRNA. (4) This assay may be implemented isothermally without the involvement of expensive complicated instruments.[23] Taking advantage of the high efficiency of DSN/TdT-mediated cascade signal amplification and enhanced fluorescence signal of G-quadruplex/ThT complexes, this biosensor exhibits high sensitivity with a LOD of 3.03×10^{-17} M and a wide linear range over 7 orders of magnitude. Importantly, this biosensor can discriminate target circRNA from one-base mismatched circRNA and exhibit good performance in human serum. Moreover, it can accurately detect circRNA in cancer cells at a single-cell level and even differentiate the circMTO1 levels in the tissues of healthy persons and nonsmall cell lung cancer (NSCLC) patients, providing great potential for circRNA-related cancer diagnosis and therapeutics.

ASSOCIATED CONTENT

Supporting Information

The Supporting Information is available free of charge at https://pubs.acs.org/doi/10.1021/acs.analchem.2c01901.

https://doi.org/10.1021/acs.analchem.2c01901
Anal. Chem. 2022, 94, 9193−9200

Experimental details, full-length sequence of circMTO1 and its RT-qPCR primer sequences, sequences of the oligonucleotides, comparison of the assay performance using linear RNA-2, optimization of the experimental conditions, comparison of the proposed method with the reported methods for circRNA assay, detection of circRNA in the spiked human serum, fluorescence emission spectra generated by circMTO1 in cell extracts, and RT-qPCR analysis of circMTO1 in cell extracts (PDF)

AUTHOR INFORMATION

Corresponding Authors

Juan Hu − *School of Chemistry and Chemical Engineering, Southeast University, Nanjing 211189, China*; Email: hujuan@seu.edu.cn

Chun-yang Zhang − *College of Chemistry, Chemical Engineering and Materials Science, Shandong Normal University, Jinan 250014, China*; orcid.org/0000-0002-8010-1981; Email: cyzhang@sdnu.edu.cn

Authors

Shu-hua Wei − *College of Chemistry, Chemical Engineering and Materials Science, Shandong Normal University, Jinan 250014, China*

Meng Liu − *College of Chemistry, Chemical Engineering and Materials Science, Shandong Normal University, Jinan 250014, China*

Complete contact information is available at: https://pubs.acs.org/10.1021/acs.analchem.2c01901

Author Contributions

§S.-h.W. and M.L. contributed equally to this work.

Notes

The authors declare no competing financial interest.

ACKNOWLEDGMENTS

This work was supported by the National Natural Science Foundation of China (Grant No. 21735003) and the Award for Team Leader Program of Taishan Scholars of Shandong Province, China.

REFERENCES

(1) Kristensen, L. S.; Andersen, M. S.; Stagsted, L. V. W.; Ebbesen, K. K.; Hansen, T. B.; Kjems, J. *Nat. Rev. Genet.* **2019**, *20*, 675−691.
(2) Zhang, Z.; Yang, T.; Xiao, J. *EBioMedicine* **2018**, *34*, 267−274.
(3) Hansen, T. B.; Jensen, T. I.; Clausen, B. H.; Bramsen, J. B.; Finsen, B.; Damgaard, C. K.; Kjems, J. *Nature* **2013**, *495*, 384−388.
(4) Du, W. W.; Zhang, C.; Yang, W.; Yong, T.; Awan, F. M.; Yang, B. B. *Theranostics* **2017**, *7*, 4183−4191.
(5) Li, Z.; Huang, C.; Bao, C.; Chen, L.; Lin, M.; Wang, X.; Zhong, G.; Yu, B.; Hu, W.; Dai, L.; Zhu, P.; Chang, Z.; Wu, Q.; Zhao, Y.; Jia, Y.; Xu, P.; Liu, H.; Shan, G. *Nat. Struct. Mol. Biol.* **2015**, *22*, 256−264.
(6) Zhang, X. O.; Dong, R.; Zhang, Y.; Zhang, J. L.; Luo, Z.; Zhang, J.; Chen, L. L.; Yang, L. *Genome Res.* **2016**, *26*, 1277−1287.
(7) Chen, L.; Nan, A.; Zhang, N.; Jia, Y.; Li, X.; Ling, Y.; Dai, J.; Zhang, S.; Yang, Q.; Yi, Y.; Jiang, Y. *Mol. Cancer* **2019**, *18*, No. 13.
(8) Hu, C.; Wang, Y.; Li, A.; Zhang, J.; Xue, F.; Zhu, L. *J. Cell. Physiol.* **2019**, *234*, 9225−9232.
(9) Weng, W.; Wei, Q.; Toden, S.; Yoshida, K.; Nagasaka, T.; Fujiwara, T.; Cai, S.; Qin, H.; Ma, Y.; Goel, A. *Clin. Cancer Res.* **2017**, *23*, 3918−3928.
(10) Lyu, P.; Zhai, Z.; Hao, Z.; Zhang, H.; He, J. *Eur. J. Clin. Invest.* **2021**, *51*, No. e13487.
(11) Begum, S.; Yiu, A.; Stebbing, J.; Castellano, L. *Oncogene* **2018**, *37*, 4055−4057.
(12) Zhang, J.; Liu, H.; Hou, L.; Wang, G.; Zhang, R.; Huang, Y.; Chen, X.; Zhu, J. *Mol. Cancer* **2017**, *16*, No. 151.
(13) Aufiero, S.; Reckman, Y. J.; Pinto, Y. M.; Creemers, E. E. *Nat. Rev. Cardiol.* **2019**, *16*, 503−514.
(14) Fang, Y.; Wang, X.; Li, W.; Han, J.; Jin, J.; Su, F.; Zhang, J.; Huang, W.; Xiao, F.; Pan, Q.; Zou, L. *Int. J. Mol. Med.* **2018**, *42*, 1865−1874.
(15) Dube, U.; Del-Aguila, J. L.; Li, Z.; Budde, J. P.; Jiang, S.; Hsu, S.; Ibanez, L.; Fernandez, M. V.; Farias, F.; Norton, J.; Gentsch, J.; Wang, F.; Salloway, S.; Masters, C. L.; Lee, J. H.; Graff-Radford, N. R.; Chhatwal, J. P.; Bateman, R. J.; Morris, J. C.; Karch, C. M.; Harari, O.; Cruchaga, C.; et al. *Nat. Neurosci.* **2019**, *22*, 1903−1912.
(16) Lu, S.; Yang, X.; Wang, C.; Chen, S.; Lu, S.; Yan, W.; Xiong, K.; Liu, F.; Yan, J. *J. Neurochem.* **2019**, *150*, 237−248.
(17) Bayoumi, A. S.; Aonuma, T.; Teoh, J. P.; Tang, Y. L.; Kim, I. M. *Acta Pharmacol. Sin.* **2018**, *39*, 1100−1109.
(18) Tian, T.; Zhao, Y.; Zheng, J.; Jin, S.; Liu, Z.; Wang, T. *Mol. Ther.–Nucleic Acids* **2021**, *26*, 63−80.
(19) Li, S.; Teng, S.; Xu, J.; Su, G.; Zhang, Y.; Zhao, J.; Zhang, S.; Wang, H.; Qin, W.; Lu, Z. J.; Guo, Y.; Zhu, Q.; Wang, D. *Briefings Bioinf.* **2019**, *20*, 1420−1433.
(20) Dahl, M.; Daugaard, I.; Andersen, M. S.; Hansen, T. B.; Grønbæk, K.; Kjems, J.; Kristensen, L. S. *Lab. Invest.* **2018**, *98*, 1657−1669.
(21) Zhao, J.; Lee, E. E.; Kim, J.; Yang, R.; Chamseddin, B.; Ni, C.; Gusho, E.; Xie, Y.; Chiang, C. M.; Buszczak, M.; Zhan, X.; Laimins, L.; Wang, R. C. *Nat. Commun.* **2019**, *10*, No. 2300.
(22) Zheng, Q.; Bao, C.; Guo, W.; Li, S.; Chen, J.; Chen, B.; Luo, Y.; Lyu, D.; Li, Y.; Shi, G.; Liang, L.; Gu, J.; He, X.; Huang, S. *Nat. Commun.* **2016**, *7*, No. 11215.
(23) Li, T.; Shao, Y.; Fu, L.; Xie, Y.; Zhu, L.; Sun, W.; Yu, R.; Xiao, B.; Guo, J. *J. Mol. Med.* **2018**, *96*, 85−96.
(24) Zhang, P.; Guo, N.; Gao, K.; Su, F.; Wang, F.; Li, Z. *Org. Biomol. Chem.* **2020**, *18*, 3269−3273.
(25) Wu, D.; Lu, H.; Wang, J.; Wu, L.; Liu, L.; Yi, X.; Wang, J.; Tang, H. *Microchem. J.* **2021**, *164*, No. 106066.
(26) Jiao, J.; Li, C.; Ning, L.; Shi, L.; Wang, L.; Xiang, Y.; Li, G. *Sens. Actuators, B* **2020**, *302*, No. 127166.
(27) Dong, J.; Zeng, Z.; Sun, R.; Zhang, X.; Cheng, Z.; Chen, C.; Zhu, Q. *Biosens. Bioelectron.* **2021**, *192*, No. 113508.
(28) Jiao, J.; Xiang, Y.; Duan, C.; Liu, Y.; Li, C.; Li, G. *Anal. Chem.* **2020**, *92*, 12394−12399.
(29) Liu, Y.; Zhang, X.; Liu, M.; Xu, F.; Zhang, Q.; Zhang, Y.; Weng, X.; Liu, S.; Du, Y.; Zhou, X. *Anal. Chim. Acta* **2020**, *1101*, 169−175.
(30) Qu, H.; Chen, M.; Ge, J.; Zhang, X.; He, S.; Xiong, F.; Yan, Q.; Zhang, S.; Gong, Z.; Guo, C.; Wang, F.; Zeng, Z.; Li, X.; Li, G.; Xiong, W.; Wu, X. *Anal. Chim. Acta* **2022**, *1189*, No. 339210.
(31) Hu, J.; Liu, W.; Wang, J.; Qiu, J. G.; Zhang, C. Y. *Anal. Chem.* **2021**, *93*, 6913−6918.
(32) Ma, F.; Wei, S. H.; Leng, J.; Tang, B.; Zhang, C. Y. *Chem. Commun.* **2018**, *54*, 2483−2486.
(33) Hu, J.; Liu, M. H.; Zhang, C. Y. *Chem. Sci.* **2018**, *9*, 4258−4267.
(34) Li, C. C.; Hu, J.; Luo, X.; Hu, J.; Zhang, C. Y. *Anal. Chem.* **2021**, *93*, 14568−14576.
(35) Ter-Ovanesyan, D.; Gilboa, T.; Lazarovits, R.; Rosenthal, A.; Yu, X.; Li, J. Z.; Church, G. M.; Walt, D. R. *Anal. Chem.* **2021**, *93*, 5365−5370.
(36) Fan, L.; Chong, X.; Zhao, M.; Jia, F.; Wang, Z.; Zhou, Y.; Lu, X.; Huang, Q.; Li, P.; Yang, Y.; Hu, Z.; Li, Q.; Zhang, X.; Shen, L. *Anal. Chem.* **2021**, *93*, 665−670.
(37) Zhang, Y.; Wang, C.; Zou, X.; Tian, X.; Hu, J.; Zhang, C. Y. *Nano Lett.* **2021**, *21*, 4193−4201.
(38) Li, C. C.; Chen, H. Y.; Luo, X.; Hu, J.; Zhang, C. Y. *Chem. Sci.* **2021**, *12*, 12407−12418.
(39) Zhao, S. J.; Zheng, P.; Wu, Z.; Jiang, J. H. *Anal. Chem.* **2022**, *94*, 2693−2698.

(40) Jeck, W. R.; Sharpless, N. E. *Nat. Biotechnol.* **2014**, *32*, 453−461.
(41) Liu, J.-B.; Yang, C.; Ko, C.-N.; Kasipandi, V.; Yang, B.; Lee, M.-Y.; Leung, C.-H.; Ma, D.-L. *Sens. Actuators, B* **2017**, *243*, 971−976.
(42) Wang, M.; Wang, W.; Kang, T. S.; Leung, C. H.; Ma, D. L. *Anal. Chem.* **2016**, *88*, 981−987.
(43) Wang, W.; Yung, T.-L.; Cheng, S.-S.; Chen, F.; Liu, J.-B.; Leung, C.-H.; Ma, D.-L. *Sens. Actuator B-Chem.* **2020**, *321*, No. 128486.
(44) Jansson, L. I.; Hentschel, J.; Parks, J. W.; Chang, T. R.; Lu, C.; Baral, R.; Bagshaw, C. R.; Stone, M. D. *Proc. Natl. Acad. Sci. U.S.A.* **2019**, *116*, 9350−9359.
(45) Han, D.; Li, J.; Wang, H.; Su, X.; Hou, J.; Gu, Y.; Qian, C.; Lin, Y.; Liu, X.; Huang, M.; Li, N.; Zhou, W.; Yu, Y.; Cao, X. *Hepatology* **2017**, *66*, 1151−1164.
(46) Chen, M.; Ai, G.; Zhou, J.; Mao, W.; Li, H.; Guo, J. *Biomed. Pharmacother.* **2019**, *117*, No. 109064.
(47) Wang, X.; Lin, Y. K.; Lu, Z. L.; Li, J. *Eur. Rev. Med. Pharmacol. Sci.* **2020**, *24*, 8359−8366.
(48) Szabo, L.; Salzman, J. *Nat. Rev. Genet.* **2016**, *17*, 679−692.
(49) Suzuki, H.; Zuo, Y.; Wang, J.; Zhang, M. Q.; Malhotra, A.; Mayeda, A. *Nucleic Acids Res.* **2006**, *34*, No. e63.
(50) Yin, B. C.; Liu, Y. Q.; Ye, B. C. *J. Am. Chem. Soc.* **2012**, *134*, 5064−5067.
(51) Wang, L. J.; Liu, H.; Zou, X.; Xu, Q.; Zhang, C. Y. *Anal. Chem.* **2021**, *93*, 10704−10711.
(52) Mohanty, J.; Barooah, N.; Dhamodharan, V.; Harikrishna, S.; Pradeepkumar, P. I.; Bhasikuttan, A. C. *J. Am. Chem. Soc.* **2013**, *135*, 367−376.
(53) Zhang, B.; Chen, M.; Jiang, N.; Shi, K.; Qian, R. *Cancer Biol. Ther.* **2019**, *20*, 1127−1135.

https://doi.org/10.1021/acs.analchem.2c01901
Anal. Chem. 2022, 94, 9193−9200